Analecta Technica Szegedinensia
Vol. 17, No. 2 ISSN 2064-7964 2023

MARKERLESS MEASUREMENT TECHNIQUES FOR MOTION ANALYSIS IN SPORTS SCIENCE

Yao Meng[1,2], István Bíró[2], József Sárosi[2]*

[1] Doctoral School on Safety and Security Sciences, Óbuda University, Népszínház street 8. 1081, Budapest, Hungary
[2]Faculty of Engineering, University of Szeged, Mars tér 7. 6724, Szeged, Hungary
*e-mail: jymengyao@gamil.com

ABSTRACT

Markerless motion capture system and X-ray fluoroscopy as two markerless measurement systems were introduced the application method in sports biomechanical areas. An overview of the technological process, data accuracy, suggested movements, and recommended body parts were explained. The markerless motion capture system consists of four parts: camera, body model, image feature, and algorithms. Even though the markerless motion capture system seems promising, it is not yet known whether these systems can be used to achieve the required accuracy and whether they can be appropriately used in sports biomechanics and clinical research. The biplane fluoroscopy technique analyzes motion data by collecting, image calibrating, and processing, which is effective for determining small joint kinematic changes and calculating joint angles. The method was used to measure walking and jumping movements primarily because of the experimental conditions and mainly detect the data of lower limb joints.

Keywords: markerless measurement, motion analysis, biomechanics

1. INTRODUCTION

Sports biomechanics settings have made important advances in the study of human movement from manual digitizing to marker-based motion capture systems, markerless systems with various computer technology. The most common method of collecting biomechanical data is by using markers. Nevertheless, it is susceptible to an intrinsic shortage of data error as a result of skin movement artifacts caused by the markers[1]. An accurate 3D kinematic analysis of bones can only be achieved through invasive methods, such as intracortical pins[2]. Markerless motion capture systems offer promise as a result of a variety of recent technological advancements. Radiographic techniques such as X-ray fluoroscopy provide an accurate measure of skeletal kinematics[3]. The purpose of this review is to provide an overview of how these two technologies can be used and provide accuracy advice and application recommendations.

2. MATERIALS AND METHODS

2.1. Markerless motion capture system based on computer vison approach

The markerless motion capture system consists of four parts： camera, body model, image feature, and algorithms. The camera systems used in such applications are usually active cameras equipped with depth-sensing capabilities, such as the most well-known Microsoft's Kinect[4]. The advantages of these types of cameras over traditional cameras are that they have a lower impact on lighting and can be used in outdoor experiment environments. The active cameras rely on two different technologies: structured light as used in Kinect and time-of-flight as used in Kinect 2. Time-of-flight devices measure the time for a pulse of light to return to the camera, as opposed to Structured Light devices which use deformations of known patterns. Several studies have been published previously using active cameras in sports biomechanics; however, the currently active camera technology has limitations regarding the precision of the biomechanics data collected[5].
Instead of a manual marker method, the markerless camera system uses body models to represent the human body. The body model can either be regarded as an accurate representation of the skeleton, based on lengths of bones and joints position, or as a shape that is derived from the external surface but has questions affecting

the skeleton[6]. But there still is the problem of optimal data by the algorithms which influence the data's actual accuracy.

A body's position and pose can be accurately determined using a markerless motion capture system, which extracts “features” from the captured image based on pixels related to the object. Image silhouettes were used as the key method of analyzing images, but recent development has moved the method to body models, which improve robustness and reduce ambiguity[7]. There is, however, no precision information regarding biomechanics kinematics data because it only detects body pose.

Generative algorithms base on the information extracted from the image and the pose and shape of the real body is determined by fitting a body model to the information[7, 8]. Then compare the model parameters to the extracted body data, which aim to determine the difference. However, the discriminative approaches do not use body models. Discriminative approaches train systems to identify body motions through deep learning or by using exemplar data whose poses are sufficiently known[9].

2.2. X-ray fluoroscopes

By using X-ray images, radiostereometric analysis (RSA) allows the reconstruction of 3D positions of objects in space. The use of biplane fluoroscopy without markers has been validated as an effective means to determine accurate skeletal kinematics. Two X-ray fluoroscopes with 9-inch image intensifiers (SIREMOBIL Compact-L mobile C-arms, Siemens Medical Solutions Canada Inc., Mississauga, Canada) were used in most studies. Data collection, calibration, and data processing are the three components of this X-ray motion capture analysis system.

Data collection: during the trials, participants have to wear radiation protection suits. Biplane fluoroscopes would have a relative angle between 90 and 135 degrees[10], thus maintaining the accuracy of the fluoroscopic video. Therefore, fluoroscopes could be placed at an angle to best suit the research requirements by changing their position. Nevertheless, the range of the relative angle is limited, and the fluoroscopy equipment is large so that the movement category can only be detected to a limited extent with matters that need attention. The left foot, for example, should avoid the fluoroscope if the right foot is what needs to be detected. In addition to the fluoroscopy video, computed tomography (CT) may also be required at the same body part to build a 3D model.

Calibration: Fluoroscopic images, which are produced with microelectrons, have the primary aberrations as conventional light images. Fluoroscopic images suffer from mainly three modes of image distortion which are pincushion, S-shape, and spiral distortion. To calibrate the image distortion, a frame using orthogonal control planes and fiducial planes is used.

An image intensifier is temporarily placed in front of a grid of beads to quantify how much distortion there is present before performing distortion correction. For example, the pincushion distortion can be calibrated by installing a distortion grid on the image intensifier during the data collection process. The MATLAB software and algorithm are utilized to determine fluoroscopy and image plane parameters, including manually locating the position of the beads and reconstructing the experiment set up, including discovering the coordinate system and establishing individual foci.

Data processing: Using image processing software (such as DICOM) create the 3D model based on the CT images. Choose two frames from the X-ray video taken with fluoroscopic equipment at the moment the aim movement is occurring. The following is manually matched 3D models to the relative position in the two frame images. Then the angel of the matched model will be calculated in the experiment set up construction in software.

DOI: 10.14232/analecta.2023.2.24-31

Analecta Technica Szegedinensia
Vol. 17, No. 2 ISSN 2064-7964 2023

3. RESULTS AND DISCUSSION

3.1. Accuracy and application recommendation

By using markerless motion analysis, it is possible to reduce joint angle measurement error compared to marker-based systems. Nonetheless, the error caused by skin or soft tissue movement is difficult to compare, as the markerless motion analysis technique for biomechanics has relatively low precision[11].

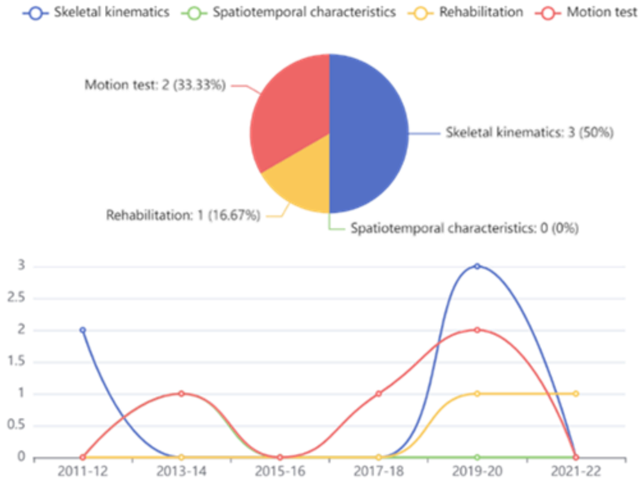

Figure 1. The pie chart, showing the Kinect research distribution at four different sports biomechanics areas in 2019-2020 which data based on the Table 1. The line chart, showing the overview of the fluctuation of Kinect research in sports biomechanics areas from 2011 to 2022 which data based on the Table 1.

As well, it remains difficult for a markerless motion system to detect some joint's rotation, such as ankle and knee joints, in the transverse plane accurately standards for markerless. The measurement error will change depending upon the type of movement, the participants, and the environment, so there is no common accuracy motion analysis. Nevertheless, the markerless motion capture analysis system may provide information that will help form training plans for applied fields by allowing step frequency and step length when analyzing gait, but as shown the researches in Table 1 and Figure 1, which are mainly focus on skeletal kinematics for comparative research with Vicon and motion tests areas.

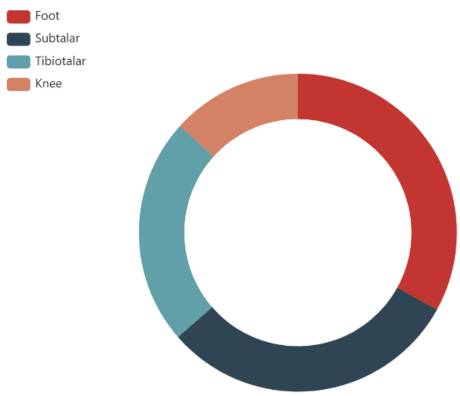

Figure 2. The pie chart shows the research weight of dual fluoroscopes analysis in the lower limb joint, which data is based on Table 2.

DOI: 10.14232/analecta.2023.2.24-31

Analecta Technica Szegedinensia

Vol. 17, No. 2 ISSN 2064-7964 2023

Table 1. Characters of paper used markerless method

	Participants	Movement	Outcome measure	Orientation/distance	Data type	Gold standard	Reliable
Ceseracciu et al.2011 [23]	5 sprint swimmers, Age 22.8±2.2	Front crawl swimming	Three dimensional coordinates of shoulder, elbow and wrist joints centers	Six underwater color analog wide-angle cameras	Depth data	SIMI Reality Motion Systems GmbH	Wrist joint (RMSD<56 mm),
Dar et al.2019 [22]	n=48, Healthy, Age: 28.45±5.61 years	Jump-landing	The landing error scoring system (LESS)	One Kinect sensor, 1.5m	Depth data	Two 30Hz video cameras 3.4m	Mean LESS of video and the · PhysiMax· was 4.77 (±2.29) and 5.15 (±2.58), respectively, (ICC = 0.80, 95% CI, 0.65–0.87), mean absolute differences 1.13 (95% CI, 0.79–1.46).
Mauntel et al.2021 [21]	n=20, Healthy, (10M,10F), Age: 20.50± 2.78	Jump-landing	Sagittal and frontal plane trunk, hip joint, and knee joint angles	One Kinect sensor, 3.4m in front of the subject	Depth data	200 Hz Vicon system 3D motion analysis	Agreement existed between the systems (ICC range = −1.52 to 0.96; ICC average = 0.58), with 75.00% (n = 24/32) of the measures being validated (P ⩽ .05). Agreement was better for sagittal- (ICC average = 0.84) than frontal- (ICC average = 0.35) plane measures.
Eltoukhy et al.2017 [20]	n=10, Healthy(5M,5F)	Balance test	Star excursion balance test	One Kinect sensor, 2.5m	Skeletal data	Eight infrared cameras	Lower limb kinematics of less than 5°, except for the knee frontal-plane angle (5.7°) in the posterior-lateral direction
Cai et al.2019 [19]	n=10M, Healthy	Upper limb movement	Shoulder, elbow	One Kinect sensor, 2m	Skeletal data	100Hz Vicon system 3D motion analysis	Shoulder and elbow flexion/extension angular waveforms (CMC>0.87), shoulder adduction/abduction angular waveforms (CMC=0.69-0.82)
Fern'ndez-Baena et al.2012 [18]	/	Flexion /extension , adduction/abduction	Knee, hip, shoulder	One sensor, 2m	Skeletal data	120Hz camera	All knee degree error are lower than 10° ranging from 6.78° to 8.98; hip errors in sagittal movements are lower than the other cases, however errors in coronal plane are lower than 10°; shoulder results are varying between 7° to 13° in all plane rotations
Clark et al.2013 [17]	n=21, Healthy, Age: 26.9±4.5	Walking	Spatiotemporal gait variables	One Kinect sensor, 1,8-3.5m	Skeletal data	120 Hz Vicon system 3D motion analysis	Gait speed, step length and stride length (r and rc values >0.90). Foot swing velocity (r=0.93. Step time (r=0.82 and rc=0.23) and stride time (r=0.69 and rc=0.14)
Ma et al.2020 [16]	n=5, Healthy(2M,3F), Age: 29.8±5.8	Walking	Hip, knee, and ankle angles	Two Kinect sensor at 4m	Depth data	100Hz Vicon system 3D motion analysis	The dual Azure Kinect provide accurate knee angles (CMC=0.87±0.06, RMSE=11.9°±3.4°), hip sagittal angles (CMC=0.60±0.34, RMSE=15.1°±6.5°). The hip frontal, transversal, and ankle angles demonstrated poor validity.
Sandau et al. 2014[15]	n=10, Healthy	Walking	Hip, knee, ankle kinematics	Eight 75Hz Camera Link cameras	Depth data	With 9 markers	The variability between trials was similar for the markerless and the marker based system with a slight exception of knee IE and ankle valgus/varus
Wochatz et al.2019 [14]	n=21, Healthy (13F, 8M), Age: 40 ± 14	Lower limb rehabilitation (squat, hip abduction and lunge exercises)	Abduction/adduction; flexion/extension (knee, hip)	One Kinect sensor, 2.5m	Skeletal data	500Hz Vicon system 3D motion analysis	Overestimations by the Kinect were apparent for hip flexion during the squat and hip abduction/adduction during the hip abduction exercise as well as for the knee positions during the lunge. Knee and hip flexion during hip abduction and lunge were underestimated by the Kinect.
Çubukçu et al.2021 [13]	29 shoulder damaged volunteers	Rehabilitation (shoulder)	Abduction, flexion, extension exercises and starting positions	One Kinect sensor and Physiotherapy Mentor Application, 2m	Skeletal data	Traditional method	While the limitations of patients using the proposed Kinect-based treatment system decreased by 30.42%, the limitations of patients who were treated with the traditional method decreased only 13.87%.
Schmitz et al.2014[12]	A jia	Motion simulation	Jig flexed, adducted, and internally rotated.	One Kinect sensor	Depth data	200Hz Motion Analysis	The systems agreed with each other by <0.5° for sagittal and frontal plane joint angles and <2° for transverse plane rotation. Both systems showed a coefficient of reliability <0.5° for all angles.

DOI: 10.14232/analecta.2023.2.24-31

Table 2. Characters of paper used Radiostereometric method

	Participants	Movement	Biplane radiographs joints/body parts	Outcome measure	Relative angle of dual fluoroscopic	Gold standard	Accuracy/result
Kessler et al.2019 [30]	n=9, Healthy(6M, 3F)	Walking and running	Foot and Ankle	Foot and Ankle Kinematics	130 degree	250Hz Qualysis system 3D motion analysis	Sagittal plane angles were in good agreement (ankle: R2 = 0.947, 0.939; Medial Longitudinal Arch (MLA) Angle: R2 = 0.713, 0.703, walking and running, respectively)
Campbell et al.2016 [29]	6M,recreational athletes, Age:37.8 ± 8.6	Walking(Barefoot and shoe condition)	Ttibia and calcaneus	Translation and rotation of the calcaneus relative to the tibia	Not shown	/	Peak plantarflexion was higher (barefoot: 9.1° ; 95 % CI 5.2:13.0; shod: 5.7° ; 95 % CI 3.6:7.8; p = 0.015) during barefoot walking compared to shod walking.
Hoffman et al.2015 [28]	n=12, recreational runners(6M,6F,Age 24.2± 4.4	Running (three conditions: Barefoot, minimalist, MC)	Foot	Magnitude and rate of navicular drop avicular drop	Not shown	/	Footwear condition was not found to have a significant effect on the magnitude of navicular drop (p = 0.22), but motion control shoes had a slower navicular drop rate than running barefoot (p = 0.05) or in minimalist shoes (p = 0.05).
Peltz et al.2014 [27]	n=12, recreational runners(6M,6F,Age: 24.2 ±4.4	Running (three footwear conditions: Barefoot, MC,FREE)	Tibiotalar and subtalar	Rotations of the tibiotalar and subtalar joints	Not shown	/	The MC condition demonstrated significant differences compared to FREE at several points throughout the early stance phase at the subtalar joint, with the greatest differences seen at 30% in PF/DF (MC −1.4±8.8° : FREE: −0.5±9.0°), IN/EV (MC −8.1±5.7° : FREE −6.3±5.5°) and IR/ER (MC −9.5±5.3° : FREE: −8.7±5.2°).
Nichols et al.2016 [26]	n=10,Healthy (5M,5F), Age: 30.9 ± 7.2	Treadmill walking and a balanced, single-leg heel-rise	Tibiotalar and subtalar	Dorsiflexion/plantarflexion and inversion/eversion,	Not shown	250-300Hz Vicon system 3D motion analysis	Differences between vicon model and dual-fluoroscopy measurements were highly variable across subjects, with joint angle errors in at least one rotation direction surpassing 10° for 9 out of 10 subjects.
Pitcairn et al.2018 [25]	n=4, ACR-L surgery, (1M, 3F, Age: 24 ±4	Over ground walking and stair ascent	Patella, femur, and tibia	Translations and rotations (joint kinematics)	55 degree	RSA	The differences increased by 34% and 40%, respectively, when the patella was at least partially obstructed by the contralateral leg.
Uzuner et al.2019 [24]	One female, age:24,weight: 59,; one male,age:25, weight:68	Prolonged standing(10 mins)	Knee	Tibiofemoral joints relative angles and displacements for creep response	Not shown	/	The maximum anterior-posterior translations during 10-min standing were approximately 4 mm for both participants, although one showed better stability than the other.

The dual fluoroscopes analysis could directly track bones by radiographic techniques to obtain foot and glenohumeral joint kinematics, which is challenging for markers motion camera capture as they have skin movement errors. This motion analysis method has advantages in determining the small joint kinematics changes and joint angle calculation, which showed relative researches in Table 2. and Figure 2.. A sagittal plane measurement of the foot is appropriate for a radiostereometric analysis such as medial arch angle[31], navicular drop, and calcaneal inclination and the transverse plane such as talus-navicular coverage angle[32]. As a result of the experiment conditions, the method was used to primarily measure walking and jumping

DOI: 10.14232/analecta.2023.2.24-31

movements. Furthermore, it is a method that has high accuracy in identifying various foot types of joint changes[33] and orthosis intervention[34].

4. CONCLUSIONS

Motion analysis systems used in sports biomechanics must have high accuracy to detect subtle motion changes. Even though the markerless motion capture system seems promising, it is not yet known whether these systems can be used to achieve the required accuracy and whether they can be appropriately used in field-based settings (with more external validity). Although the RSA has been validated on its ability to detect subtle biomechanical data changes, it is also subject to limitations in the category of movement.

5. DISCLOSURE OF CONFLICT OF INTEREST

None

REFERENCES

[1] R. Shultz, A.E. Kedgley, T.R. Jenkyn, Quantifying skin motion artifact error of the hindfoot and forefoot marker clusters with the optical tracking of a multi-segment foot model using single-plane fluoroscopy, Gait & posture, 34 (1) (2011), pp. 44-48.
[2] A. Peters, B. Galna, M. Sangeux, M. Morris, R. Baker, Quantification of soft tissue artifact in lower limb human motion analysis: a systematic review, Gait & posture, 31 (1) (2010), pp. 1-8.
[3] J. M. Iaquinto, R. Tsai, D. R. Haynor, M. J. Fassbind, B. J. Sangeorzan, W. R. Ledoux, Marker-based validation of a biplane fluoroscopy system for quantifying foot kinematics, Medical engineering & physics, 36 (3) (2014), pp. 391-396.
[4] S. L. Colyer, M. Evans, D. P. Cosker, A. I. T. Salo, A Review of the Evolution of Vision-Based Motion Analysis and the Integration of Advanced Computer Vision Methods Towards Developing a Markerless System, Sports Med Open, 4 (1) (2018), pp. 24.
[5] S. X. M. Yang, M. S. Christiansen, P. K. Larsen, T. Alkjær, T. B. Moeslund, E. B. Simonsen, N. Lynnerup, Markerless motion capture systems for tracking of persons in forensic biomechanics: an overview, Computer Methods in Biomechanics and Biomedical Engineering: Imaging & Visualization, 2 (1) (2014), pp. 46-65.
[6] C. Stoll, N. Hasler, J. Gall, H. Seidel, C. Theobalt, Fast articulated motion tracking using a sums of gaussians body model, 2011 International Conference on Computer Vision, IEEE, November 2011, pp. 951-958.
[7] S. Corazza, L. Mündermann, E. Gambaretto, G. Ferrigno, T. P. Andriacchi, Markerless motion capture through visual hull, articulated icp and subject specific model generation, International journal of computer vision, 87 (1) (2010), pp. 156-169.
[8] S. Corazza, L. Muendermann, A. M. Chaudhari, A markerless motion capture system to study musculoskeletal biomechanics: visual hull and simulated annealing approach, Annals of biomedical engineering, 34 (6) (2006), pp. 1019-1029.
[9] C. Hong, J. Yu, Y. Xie, X. Chen, Multi-view deep learning for image-based pose recovery[C]//2015 IEEE 16th International Conference on Communication Technology (ICCT), IEEE, October 2015, pp. 897-902.
[10] A. E. Kedgley, T. R. Jenkyn, RSA calibration accuracy of a fluoroscopy‐based system using nonorthogonal images for measuring functional kinematics, Medical physics, 36 (7) (2009), pp. 3176-3180.
[11] E. Ceseracciu, Z. Sawacha, C. Cobelli, Comparison of markerless and marker-based motion capture technologies through simultaneous data collection during gait: proof of concept, PloS one, 9 (3) (2014), pp. e87640.

DOI: 10.14232/analecta.2023.2.24-31

[12] A. Schmitz, M. Ye, R. Shapiro, R. Yang, B. Noehren, Accuracy and repeatability of joint angles measured using a single camera markerless motion capture system, Journal of biomechanics, 47 (2) (2014), pp. 587-591.
[13] B. Çubukçu, U. Yüzgeç, A. Zileli, R. Zileli, Kinect-based integrated physiotherapy mentor application for shoulder damage, Future Generation Computer Systems, 122 (2021), pp. 105-116.
[14] M. Wochatz, N. Tilgner, S. Mueller, S. Rabe, S. Eichler, M. John, H. Völler, F. Mayer, Reliability and validity of the Kinect V2 for the assessment of lower extremity rehabilitation exercises, Gait & posture, 70 (2019), pp. 330-335.
[15] M. Sandau, H. Koblauch, T. B. Moeslund, H. Aanæs, T. Alkjær, E. B. Simonsen, Markerless motion capture can provide reliable 3D gait kinematics in the sagittal and frontal plane, Medical engineering & physics, 36 (9) (2014), pp. 1168-1175.
[16] Y. Ma, B. Sheng, R. Hart, Y. Zhang, The validity of a dual azure kinect-based motion capture system for gait analysis: a preliminary study, In 2020 Asia-Pacific Signal and Information Processing Association Annual Summit and Conference (APSIPA ASC), IEEE, December 2020, pp. 1201-1206.
[17] R. A. Clark, K. J. Bower, B. F. Mentiplay, K. Paterson, Y. Pua, Concurrent validity of the Microsoft Kinect for assessment of spatiotemporal gait variables, Journal of biomechanics, 46 (15) (2013), pp. 2722-2725.
[18] A. Fern'ndez-Baena, A. Susin, X. Lligadas, Biomechanical validation of upper-body and lower-body joint movements of kinect motion capture data for rehabilitation treatments, In 2012 fourth international conference on intelligent networking and collaborative systems, IEEE, September 2012, pp. 656-661.
[19] L. Cai, Y. Ma, S. Xiong, Validity and reliability of upper limb functional assessment using the Microsoft Kinect V2 sensor, Applied bionics and biomechanics, 2019 (2019).
[20] M. Eltoukhy, C. Kuenze, J. Oh, S. Wooten, J. Signorile, Kinect-based assessment of lower limb kinematics and dynamic postural control during the star excursion balance test, Gait & posture, 58 (2017), pp. 421-427.
[21] T. C. Mauntel, K. L. Cameron, B. Pietrosimone, S. W. Marshall, A. C. Hackney, D. A. Padua, Validation of a commercially available markerless motion-capture system for trunk and lower extremity kinematics during a jump-landing assessment, Journal of athletic training, 56 (2) (2021), pp. 177-190.
[22] G. Dar, A. Yehiel, M. Cale'Benzoor, Concurrent criterion validity of a novel portable motion analysis system for assessing the landing error scoring system (LESS) test, Sports biomechanics, 18 (4) (2019), pp. 426-436.
[23] E. Ceseracciu, Z. Sawacha, S. Fantozzi, M. Cortesi, G. Gatta, S. Corazza, C. Cobelli, Markerless analysis of front crawl swimming, Journal of biomechanics, 44 (12) (2011), pp. 2236-2242.
[24] S. Uzuner, M. L. Rodriguez, L. Li, S. Kucuk, Dual fluoroscopic evaluation of human tibiofemoral joint kinematics during a prolonged standing: A pilot study, Engineering science and technology, an international journal, 22 (3) (2019), pp. 794-800.
[25] S. Pitcairn, B. Lesniak, W. Anderst, In vivo validation of patellofemoral kinematics during overground gait and stair ascent, Gait & posture, 64 (2018), pp. 191-197.
[26] J. A. Nichols, K. E. Roach, N. M. Fiorentino, A. E. Anderson, Predicting tibiotalar and subtalar joint angles from skin-marker data with dual-fluoroscopy as a reference standard, Gait & posture, 49 (2016), pp. 136-143.
[27] C. D. Peltz, J. A. Haladik, S. E. Hoffman, M. McDonald, N. L. Ramo, G. Divine, M. Nurse, M. J. Bey, Effects of footwear on three-dimensional tibiotalar and subtalar joint motion during running, Journal of biomechanics, 47 (11) (2014), pp. 2647-2653.
[28] S. E. Hoffman, C. D. Peltz, J. A. Haladik, G. Divine, M. A. Nurse, M. J. Bey, Dynamic in-vivo assessment of navicular drop while running in barefoot, minimalist, and motion control footwear conditions, Gait & posture, 41 (3) (2015), pp. 825-829.

[29] K. J. Campbell, K. J. Wilson, R. F. LaPrade, T. O. Clanton, Normative rearfoot motion during barefoot and shod walking using biplane fluoroscopy, Knee Surgery, Sports Traumatology, Arthroscopy, 24 (4) (2016), pp. 1402-1408.
[30] S. E. Kessler, M. J. Rainbow, G. A. Lichtwark, A. G. Cresswell, S. E. D'Andrea, N. Konow, L. A. Kelly, A direct comparison of biplanar videoradiography and optical motion capture for foot and ankle kinematics, Frontiers in bioengineering and biotechnology, (2019), pp. 199.
[31] M. E. R. Balsdon, K. M. Bushey, C. E. Dombroski, M. LeBel, T. R. Jenkyn, Medial Longitudinal Arch Angle Presents Significant Differences Between Foot Types: A Biplane Fluoroscopy Study, J Biomech Eng, 138 (10) (2016).
[32] G. S. Murley, H. B. Menz, K. B. Landorf, A protocol for classifying normal-and flat-arched foot posture for research studies using clinical and radiographic measurements, Journal of foot and ankle research, 2 (1) (2009), pp. 1-13.
[33] D. R. Bonanno, K. B. Landorf, S. E. Munteanu, G. S. Murley, H. B. Menz, Effectiveness of foot orthoses and shock-absorbing insoles for the prevention of injury: a systematic review and meta-analysis, Br J Sports Med, 51 (2) (2017), pp. 86-96.
[34] M. Balsdon, C. Dombroski, K. Bushey, T. R. Jenkyn, Hard, soft and off-the-shelf foot orthoses and their effect on the angle of the medial longitudinal arch: A biplane fluoroscopy study, Prosthet Orthot Int, 43 (3) (2019), pp. 331-338.

DOI: 10.14232/analecta.2023.2.24-31